Aerosol and Air Quality Research, 17: 2522–2532, 2017

ISSN: 1680-8584 print / 2071-1409 online
doi: 10.4209/aaqr.2017.08.0271

Effects of Carbon Dioxide Addition on the Soot Particle Sizes in an Ethylene/Air Flame

Linghong Chen[1], Jianwu Zhou[1], Xianjue Zheng[2], Jian Wu[1], Xuecheng Wu[1*], Xiang Gao[1], Gérard Gréhan[3], Kefa Cen[1]

[1] *State Key Laboratory of Clean Energy Utilization, Zhejiang University, Hangzhou 310027, China*
[2] *Hangzhou Environmental Monitoring Center Station, Hangzhou 310007, China*
[3] *UMR 6614/CORIA, CNRS, BP12 76801 Saint Etienne du Rouvray, France*

ABSTRACT

Carbon dioxide (CO_2) is an important compound for the inhibition of combustion flame. This work investigated the effects of CO_2 addition on the soot particle sizes in axisymmetric laminar co-flow ethylene/air diffusion flames, as determined by using temporal laser-induced incandescence (LII). Additionally, the flame height and absorption function of soot particles were also studied. The results showed that the size and absorbency of soot particles decreases with the addition of CO_2. The total flame height also decreases with CO_2 addition, while the height of the dark region grows. These results show that CO_2 addition dilutes the gas stream, compresses the nucleation of soot particles and makes them less mature. This study provides useful information for the control of soot particle formation during combustion processes.

Keywords: Carbon dioxide dilution; Flame height; Laser-induced incandescence; Particle sizes; Absorption function.

INTRODUCTION

Reducing the emission of soot particles is of great importance, since soot particles present a significant threat to human health and accelerate the greenhouse effect (Das *et al*., 2015; Jose, 2016; Lin *et al.*, 2016; Nagy*et al*., 2016). CO_2 is one of the main components used in flue gas recirculation, which is a highly effective technique used for lowering NO_x emissions from burners. Therefore, it is necessary to find out how CO_2 dilution affects the soot particles in such flames.

Previous studies have been conducted to analyze the effects of CO_2 dilution. Generally speaking, CO_2 dilution can reduce soot formation. Earlier works mainly focus on the three effects of adding CO_2, which are dilution, temperature and direct chemical participation (Mclintock, 1968; Schug *et al*., 1980; Angrill *et al*., 2000). In more recent years most researchers have studied the influence of CO_2 dilution on soot formation directly, without analyzing the three specific effects, since Liu *et al*. (2001) claimed that it was impossible to totally isolate these three effects experimentally. Instead, they investigated the nucleation, surface growth and oxidation of soot particles. Most results showed that CO_2 dilution exerted negative effects on the nucleation of incipient soot and had nearly no effect on the oxidation of soot particles. As for the surface growth of soot particles, Oh *et al*. (2005) found no changes in the surface growth rate, while Gu *et al*. (2016) concluded in their simulation results that CO_2 dilution on the fuel side strongly reduced surface growth. Consequently, an experimental study is needed to make clear the influence of CO_2 addition on soot formation. Moreover, few studies have been carried out to investigate the influence of CO_2 dilution on the flame structure and optical properties.

Flame height has been used to test models of flame structure (D'Anna *et al*., 2002), and calculate the residence times of soot particles (Oh *et al*., 2007). It was studied by Roper (1977) and a correlation was put forward to predict the stoichiometric height of flames. Zhao *et al*. (2014) conducted their experiment by measuring flame heights with the addition of hydrogen and nitrogen to the fuel side, and found that the Roper correlation could well predict the changes in flame heights. They concluded that the flame heights should not be influenced by the addition of gases which did not participate in the chemical reaction. Wu *et al*. (2015) studied the effects of hydrogen addition on the flame heights of the dark region, and a significant increase in the soot-free length was observed with the addition of hydrogen, indicating that this reduced the carbon loading. However, to date there are no similar studies examining CO_2 dilution.

Most of the properties of soot particles are very different from those of the other kinds of particles that are generated simultaneously (Pu *et al*., 2015; Zhan *et al*., 2016), and

* Corresponding author.
Tel.: (86) 0571-87952805
E-mail address: wuxch@zju.edu.cn

closely related to their sizes (Wu *et al*., 2015; Fan *et al*., 2016). Soot particle sizes can be measured by laser-induced incandescence (LII), which has become a powerful optical diagnostic technique. In a previous study conducted by Oh and Shin (2006), the measurement of soot particle sizes was performed by applying the LII technique and sampling methods, with the results showing that the sizes measured by both methods were in good agreement. They divided diffusion flames into three regions according to the changes in soot particle sizes. With the growth of soot particles, soot particle sizes stayed nearly the same in the inception region, increased in the surface growth region and decreased in the oxidation region. These findings are now commonly used to analyze soot formation.

If we are to analyze the incandescence signal or make use of other soot optical diagnostic measurements, then it is essential to first know the optical properties of soot. For the LII measurements, determination of the soot absorption function, E(m), is significant, since this can cause significant uncertainties with regard to the simulation results of LII models (Bladh *et al.*, 2011). Previous studies found that the absorption function is positively related to the maturity of soot particles (Wang, 2011; Barone *et al*., 2003), thus indicating that the change in soot maturity could be obtained by studying the absorption function. In order to accurately analyze this previous works plotted LII fluence curves, which reflect the relation between the heating laser fluence and peak LII signals. Olofsson (2015) observed LII fluence curves plotted from a premixed flat flame, and concluded that soot particles were more transparent at lower flame heights. Migliorini *et al*. (2015) pointed out that the initial temperature of soot particles in flames exerted an influence on the fluence curves, which was also noted by Liu *et al*. (2006). However, to date no studies has been performed to analyze the effects of CO_2 dilution on the optical properties of soot.

In the current work, the study of CO_2 dilution was conducted according to the three aspects mentioned above. The luminous flame height as well as the soot-free region height were thus measured to find out how CO_2 dilution influences the flame structure. The optical properties and sizes of soot particles were analyzed by LII measurements to investigate the effects on soot formation.

METHODS

The soot generation system is shown in Fig. 1.

Laminar diffusion co-flow flames were produced by a Santoro burner consisting of two concentric tubes with inner diameters of 11.1 and 101 mm. The mixture fuel of CO_2 and ethylene passed through the inner tube while the air provided by a compressor passed between the two tubes, which contained packed beds of glass beads and porous ceramic honeycomb. The burner was placed on a three-dimensional translating stage system so that the position of the flame produced by the burner could be located and altered precisely. The flow rate conditions for the laminar diffusion co-flow flames fueled with ethylene and CO_2 of different volumetric fractions, as presented in Table 1, were controlled by the mass flow controllers (Alicat Scientific, Inc.). The flow rates of air and ethylene remained at 43 L min^{-1} and 0.15 L min^{-1} during the process of all experiments.

Flame Height Measurements

Pictures of flames were recorded using a digital camera (Nikon, D700). The ISO was set to 200 and the white balance was set to “direct sunlight” to reduce the influence on the flame luminosity. Before taking pictures of flames, a picture of a ruler placed right above the burner was taken to figure out the spatial resolution. To make sure that flames could be clearly seen in the pictures, a suitable shutter time was set for each flame, as shown in Table 1. Flame heights were determined by finding the corresponding pixel to the threshold value of luminance from each flame, which will be demonstrated later.

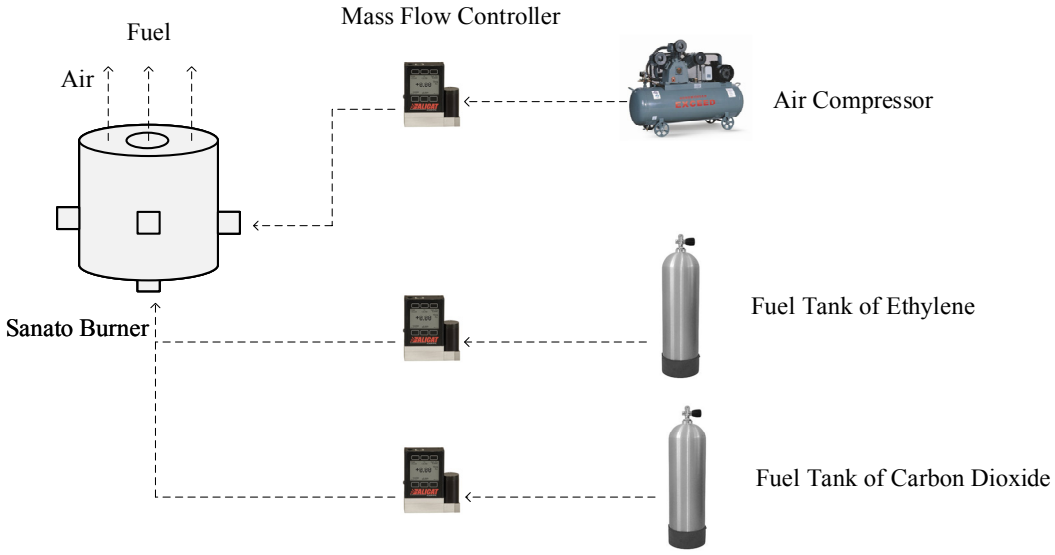

Fig. 1. Soot generation system.

Table 1. Flow rate conditions Fuel side.

X_{CO_2} (%)	Q_{CO_2} (slpm)	$Q_{C_2H_4}$ (slpm)	Q_{air} (slpm)	T_s (sec)
0	0			1/500
30	0.064	0.15	43	1/500
50	0.15			1/250

Note: X_{CO_2} is the volumetric fraction of CO_2 in the fuel.
Q_{CO_2} is the volumetric flow rate of CO_2.
$Q_{C_2H_4}$ is the volumetric flow rate of ethylene.
Q_{air} is the volumetric flow rate of air.
T_s is the shutter time set in the camera.

LII Measurements

The experimental setup and the analysis of the LII signal were based on the work conducted by Chen *et al*. (2017). The experimental setup is shown in Fig. 2.

The laser-based measurement platform consisted of laser source system, soot generation system and signal detection system. In the laser source system, a Nd/YAG laser (1064 nm) with a pulse width of 7 ns and a repetition rate of 10 Hz, was used as the excitation source to heat the soot particles in the flames. An attenuator was applied at the front of the laser to control the laser energy, which was monitored by a power meter behind the flames. Subsequently, a diaphragm was used to select the top-hat region of the laser beam where laser fluence was almost uniformly distributed. The diameter of the selected region of the laser beam was reduced to nearly 1 mm when the beam went through a telescope system consisting of two spherical lenses with diameters of 500 and 200 mm. In the signal detection system, the cylindrical probe zone with a diameter of 1 mm and a width of 1 mm in the flame was determined by a slit. The LII signals were recorded by a photomultiplier (PMT, Hamamatsu H10721-01) connected to a digital 6 GHz oscilloscope (DSO80604B). A band-pass filter at 450 nm was placed in front of the PMT to reduce the influence of flame luminosity on the LII signals.

In order to obtain LII signals with satisfying signal-to-noise ratios, the position detected in the flames should have high soot volume fraction so that the signals are strong enough. Consequently, the LII signals to be analyzed were detected at between 18 to 40 mm above the burner (HAB). The LII signals used for measurements of soot particle sizes were averaged over 128 laser shots, and the peak LII signals used for plotting fluence curves were averaged over 50 laser shots.

RESULTS AND DISCUSSION

Flame Heights

The flame heights of diffusion flames can be divided into two parts, which are the yellow luminous flame height and dark region height. The yellow color of the diffusion flames is considered to be caused by soot particles in the flames, while there are rarely soot particles in the dark region (Wu *et al*., 2015). Information about soot formation can thus be obtained through changes in the two heights.

Measurement of heights was performed by finding the uppermost pixel to cross a threshold value of luminance from each flame. The thresholds of the luminous height and dark region height were set to be twenty times and one hundred times as much as the luminance of background at the edge of each picture, respectively. Fig. 3 presents the results of the measurement of flame heights.

As shown in Fig. 3, with addition of CO_2 to the fuel side, the total flame height slightly decreased. To explain this behavior, the Roper correlation was used to simulate the total height of the flame (Roper, 1977). This correlation can predict the stoichiometric height of flames correctly, as the related equation is written as follows:

$$H = \frac{Q_F}{4\pi D_\infty In(1+1/S)}\left(\frac{T_\infty}{T_f}\right)^{0.67} \quad (1)$$

where H is the stoichiometric height (cm), Q_F is the fuel gas volumetric flow rate ($cm^3\ s^{-1}$), D_∞ is the diffusion coefficient at initial temperature ($cm^2\ s^{-1}$), S is the stoichiometric volume ratio of air to fuel, T_∞ is the initial temperature (K), which is regarded as the ambient temperature, and T_f is the temperature of the flame (K).

The stoichiometric height, also known as the height of the blue reaction region, is defined as the height of the position where the fuel and oxidizer are in stoichiometric proportions. Since it is hard to detect the blue reaction region in normal diffusion flames without using measurements of OH PLIF, researchers replace the stoichiometric height with the yellow luminous height, as they are considered to be approximate to each other (Sunderland *et al*., 2004). In this work, the stoichiometric height was thus regarded as the yellow luminous height.

When T_∞ was set to be the diffusion coefficient of ethylene in air (0.166 $cm^2\ s^{-1}$) and T_f was set to 1700K in Roper's correlation (Zhao *et al*., 2014), the height of the flame fueled with pure ethylene was calculated to be 5.18 cm, which well predicted the height of the flame, which is measured to be 5.09cm. In Fig. 3, a slight decrease in the total flame height with the addition of CO_2 was observed, and this most likely resulted from an increase in the diffusion coefficient D_∞ of the fuel, since the temperature of the flame T_f was predicted to increase, as found by Gu *et al*. (2016)

A clear trend is that the dark region height increased while the luminous region height decreased with the addition of CO_2. Since few soot particles existed in the dark region,

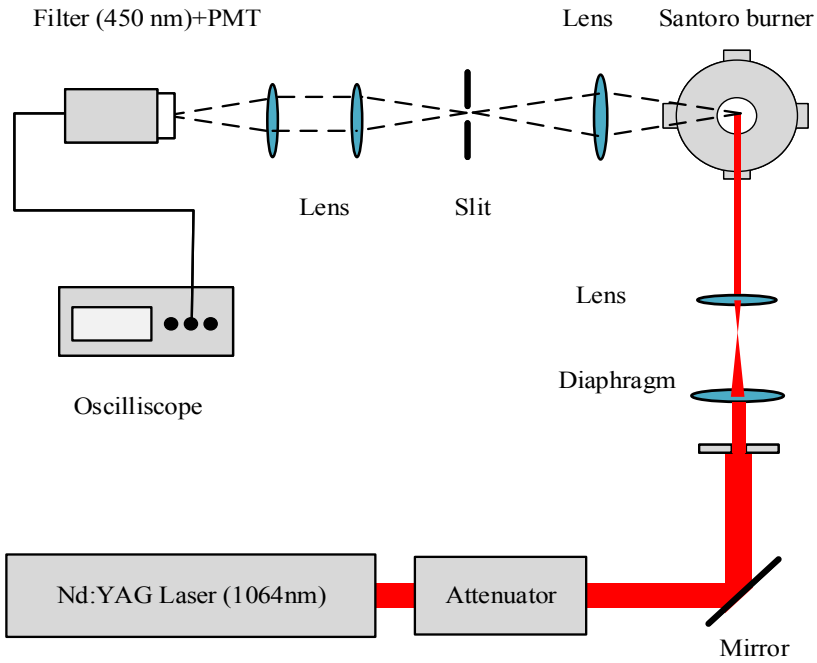

Fig. 2. The laser-based measurement platform.

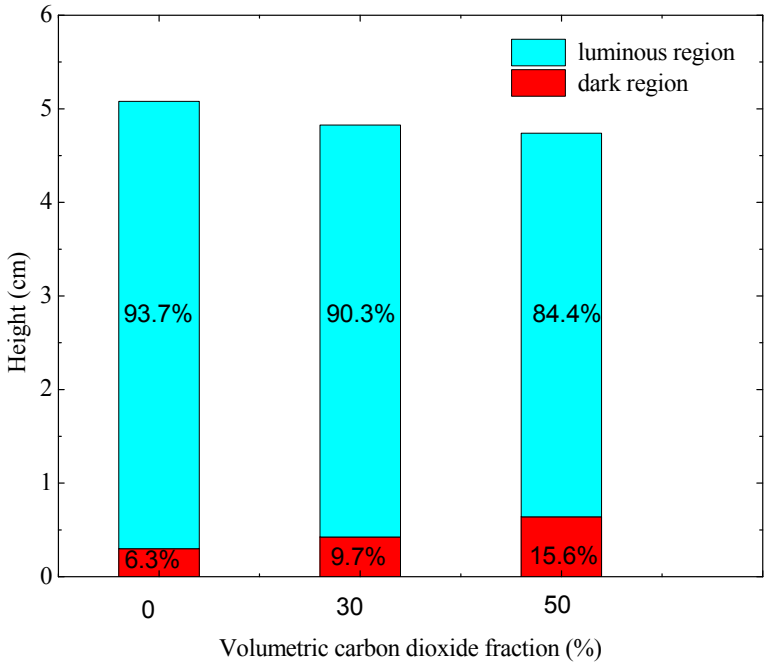

Fig. 3. The luminous heights and the dark region heights of flames.

the increase in the dark region height indicated that the formation of nascent soot began at a higher position in the flame, which suggests that the CO_2 dilution slowed down the nucleation rate. Since the total heights and shapes of the flames stayed nearly the same, the following results of the LII measurements of different flames were compared at the same position in the flame.

LII Fluence Curves

Having discussed the influence of CO_2 addition on the nucleation rates in the last section, the LII fluence curves are plotted in this section to gain information about the optical properties of soot particles.

The measurements of the LII fluence curves were carried out at four different positions in each flame. The position with 5 mm radial distance to the axis of flames at 30mm HAB was considered to be the edge of flames. The results of the measurements are shown in Fig. 5, where the curves were normalized to the strongest peak LII signal from each height.

It can be seen from Fig. 4 that all the presented curves followed the same trend that the peak LII signal increased rapidly with fluence and reached a plateau at a laser fluence higher than ~0.3 J cm^{-2}. A slight decrease in the LII signals at higher fluence can be seen in the conventional shape of the LII fluence curves, because of the sublimation of soot particles (Olofsson *et al*., 2013; Migliorini *et al*., 2015; Olofsson *et al*., 2015). However, this decrease was not found in our results, which might be caused by the fact that the top-hat profile of the laser was still not equally distributed enough, with a standard deviation of 15% observed by a beam profiler. The three presented plots showed the same trend that higher laser energy was required for the signal to reach the plateau at a lower position in the flame, indicating that higher laser energy was required for soot particles to sublimate at lower heights. This behavior could be explained by the fact that soot particles became more mature and less transparent at higher flame heights in diffusion flames, which was also found in previous studies (Smooke *et al*., 2005; Michelsen, 2017).

By comparing the fluence curves of different flames, it was found that the peak LII signal shifted slightly to a higher laser fluence with carbon-dioxide addition on the fuel side, as shown in Fig. 5. This behavior indicated that soot particles

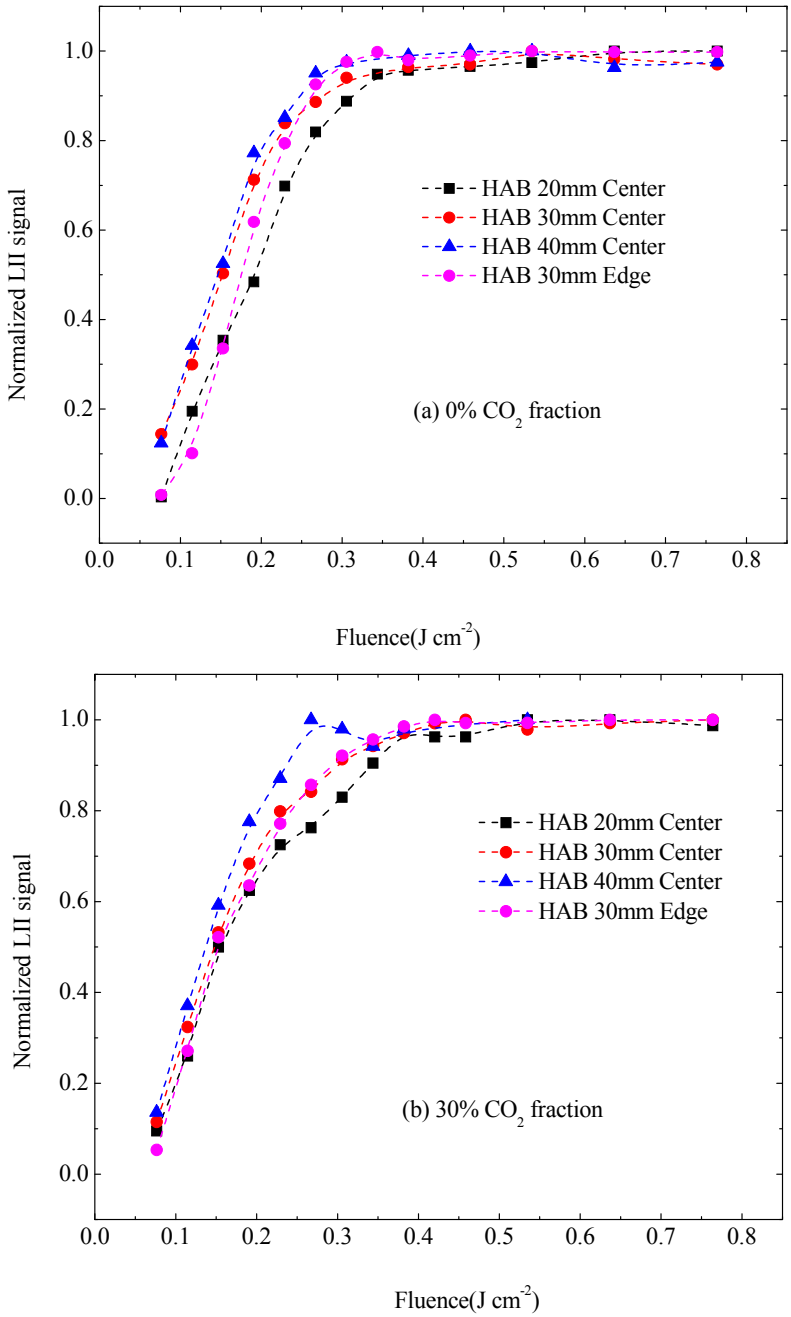

Fig. 4. LII fluence curves of flames fueled with gases containing (a) 0%, (b) 30% and (c) 50% volumetric CO_2 fraction respectively.

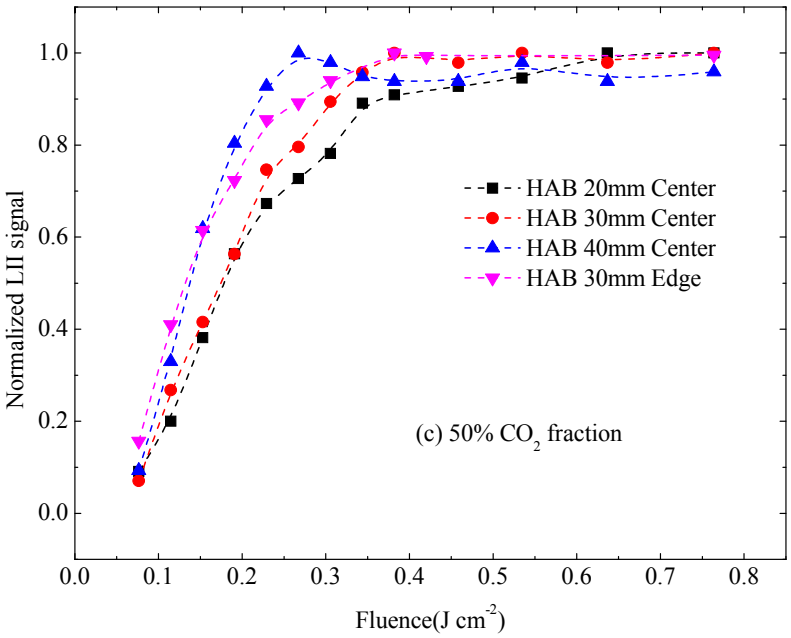

Fig. 4. (*continued*).

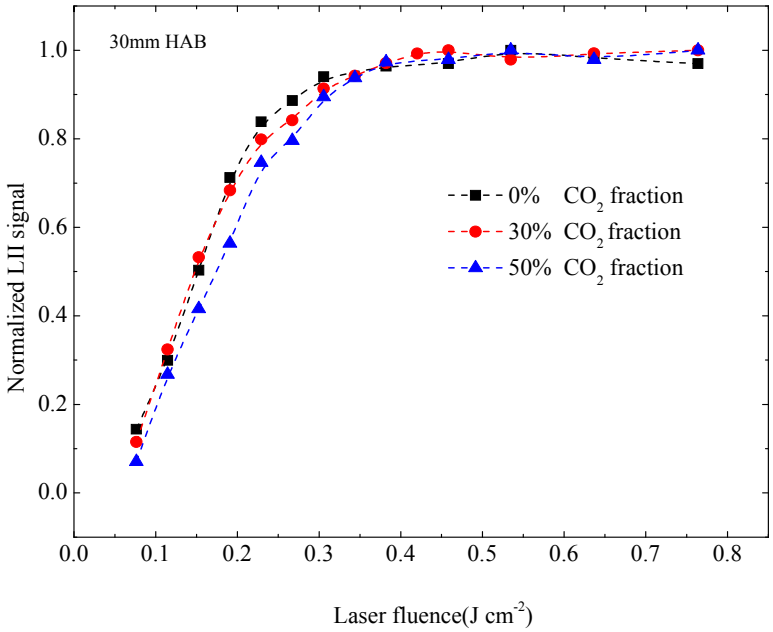

Fig. 5. The fluence curves plotted at 30 mm HAB in flames fueled with gases containing different volumetric CO_2 fractions.

became more transparent with carbon-dioxide dilution. This was in good agreement with the speculation made in the previous section that CO_2 dilution on the fuel side slowed down the growth of soot particles, making them became more nascent and with weaker absorbency at the same position in the flames.

Soot Particle Sizes

The laser fluence needs to be properly selected in order to measure the soot particle size correctly. It can be seen in Fig. 4 that the rising trend of the curves began to slow down around the fluence of 0.25 J cm^{-2}, when the sublimation of soot particles started. This fluence has two advantages for measuring particle sizes, as Sun *et al*. (2015) pointed out. The influence of sublimation on LII signals stayed low at this fluence, and the LII signals were also quite steady, since the peak temperature of the soot particles was reached around this fluence. Based on these results, the laser fluence was chosen to be 0.254 J cm^{-2} during the measurement of soot particle sizes.

A comparison of the measured LII signal decays τ derived from the experimental data with the simulated ones

based on an LII model is needed to acquire the primary particle sizes (Will *et al*., 1998; Lehre *et al*., 2003). The LII model we used in this work was demonstrated in detail in our previous work (Wu *et al*., 2017). However, while the simulated LII signals agreed well with the measured ones in the low fluences region, when applied at high fluence a difference can be found between them. This difference in the high fluence region is mainly caused by the inadequacy of the modeling of sublimation, which is still in the research stage.

The selection of the accommodation coefficient and refractive index is of great importance. In this work, the frequently used value of 0.3 is employed for the thermal accommodation coefficient, while the value of 1.56–0.46i is used for the refractive index (Schulz *et al*., 2006; Michelsen *et al*., 2007). After setting down the input parameters, including the flame temperature (1700 K), laser fluence (0.254 J cm^{-2}), excitation wavelength (1064 nm) and detection wavelength (450 nm) in the model, simulated LII signals corresponding to different primary particle sizes were obtained, as shown in Fig. 6. Previous studies pointed out that the LII decay signal was similar to an exponential function, shown as Eq. (2) (Schulz *et al*., 2006).

$$S = S_0 e^{(-\frac{t}{\tau})} \tag{2}$$

where S is the LII decay signal, and S_0 is the peak LII signal.

As mentioned above, the excitation laser fluence of this measurement was set at 0.254 J cm^{-2}, which is high enough for soot particles to sublimate. In this condition, the LII signal was mainly controlled by the rates of evaporative heat loss and mass transfer shortly after the excitation laser pulse, so it could not be fitted by an exponential function. To avoid the influence of sublimation and obtain the correct signal decays, the range of the LII decay signal for exponential fit was selected to be from 150ns to 2000ns after the excitation laser pulse, when the sublimation was almost over and the soot particle sizes were considered to be constant (Vander *et al*., 1998). Consequently, the relation between the particle size d_p and the signal decay was revealed. As shown in Fig. 7, a linear function well fitted this relation:

$$d_p = 0.153\tau - 0.507 \tag{3}$$

The measured LII signal decays τ were derived from the LII signals which were recorded by a photomultiplier connected to a digital oscilloscope. To study the effects of CO_2 addition to fuel on soot particle sizes, measurements were carried out at four different positions in the flames. Fig. 8 shows the normalized LII signals at 40 mm HAB in different flames. Signal decays were obtained in the same way as mentioned above. Applying the linear relation between signal decays and soot particle sizes, as shown as Eq. (3), the soot particle sizes were calculated, and the results are shown in Fig. 9.

Fig. 9(a) shows that adding CO_2 to the fuel side had a significant impact on decreasing particle size. This might be caused by the decrease in the nucleation rate and increase in the oxidation rate. In the previous two sections it was demonstrated that CO_2 dilution slowed down the nucleation rate of soot particles, and the effects of CO_2 dilution on the oxidation rate still need to be discussed.

The relation between soot particle sizes and their heights above the burner are revealed in Fig. 9(b). With the height increasing from 18 mm to 40 mm above the burner, the soot particle sizes increased first and then decreased. Since the soot particle sizes stayed nearly the same in the inception region, increased in the surface growth region and decreased in the oxidation region, the boundary between surface growth

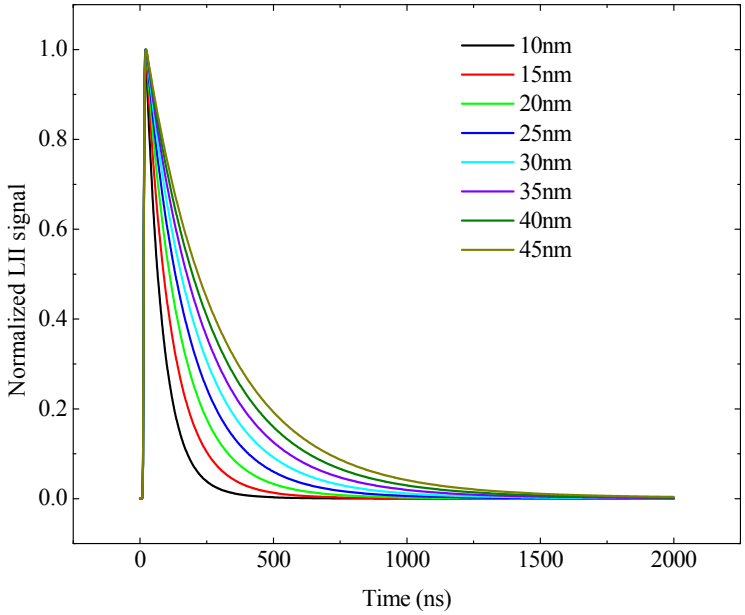

Fig. 6. Simulated LII signals of soot particles at different sizes. The input parameters were set as mentioned below.

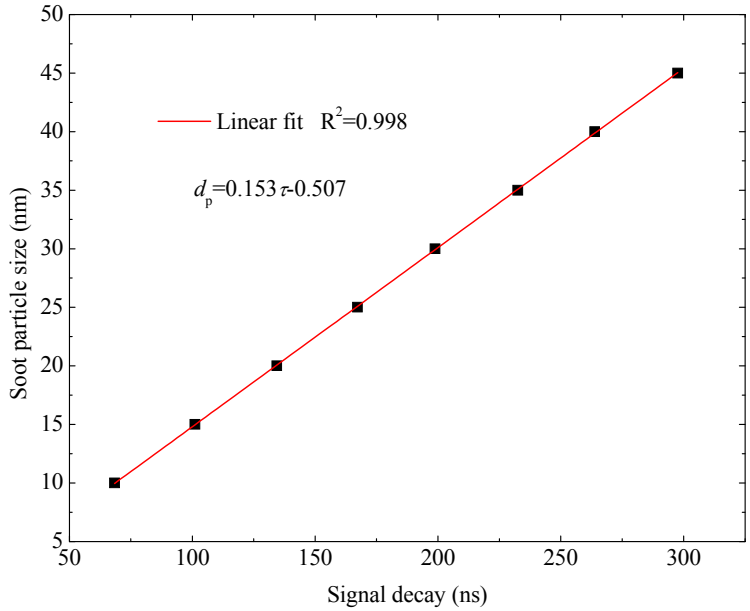

Fig. 7. The relation between the soot particle size and the signal decay. Signal decays were calculated through exponential fits to simulated LII decay signals in Fig. 6. A linear function was given to fit this relation.

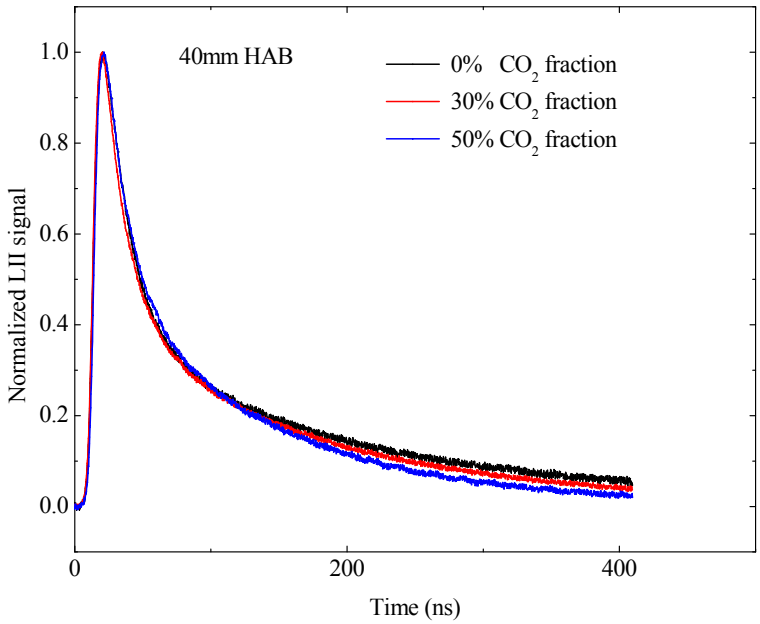

Fig. 8. Measured normalized LII signals at 40 mm HAB in different flames.

region and oxidation region can be seen from Fig. 9(b). This boundary was found to become higher with the addition of CO_2, indicating that the oxidation of soot particles started at a higher position. Since the LII signal was hard to detect and the signal-to-noise ratio was too low in positions below 18 mm HAB, the boundary between the inception region and surface growth region, as well as the surface growth rate, could not be determined. It can be seen from Fig. 9(b) that the decreasing parts of the three curves stayed nearly parallel, indicating that the addition of CO_2 had little effect on the oxidation of soot particles. Consequently, the decrease in particle sizes with CO_2 dilution was mainly caused by the decrease in the nucleation rate.

CONCLUSIONS

Addition of CO_2 to the fuel side of a laminar co-flow ethylene/air diffusion flame was studied experimentally in three regards in the current work: the flame heights, particle sizes and absorption function of soot particles. Both the luminous flame height and the dark region height were determined by using image processing. Laser-induced incandescence was applied to investigate the absorption function and sizes of soot particles. Information about the

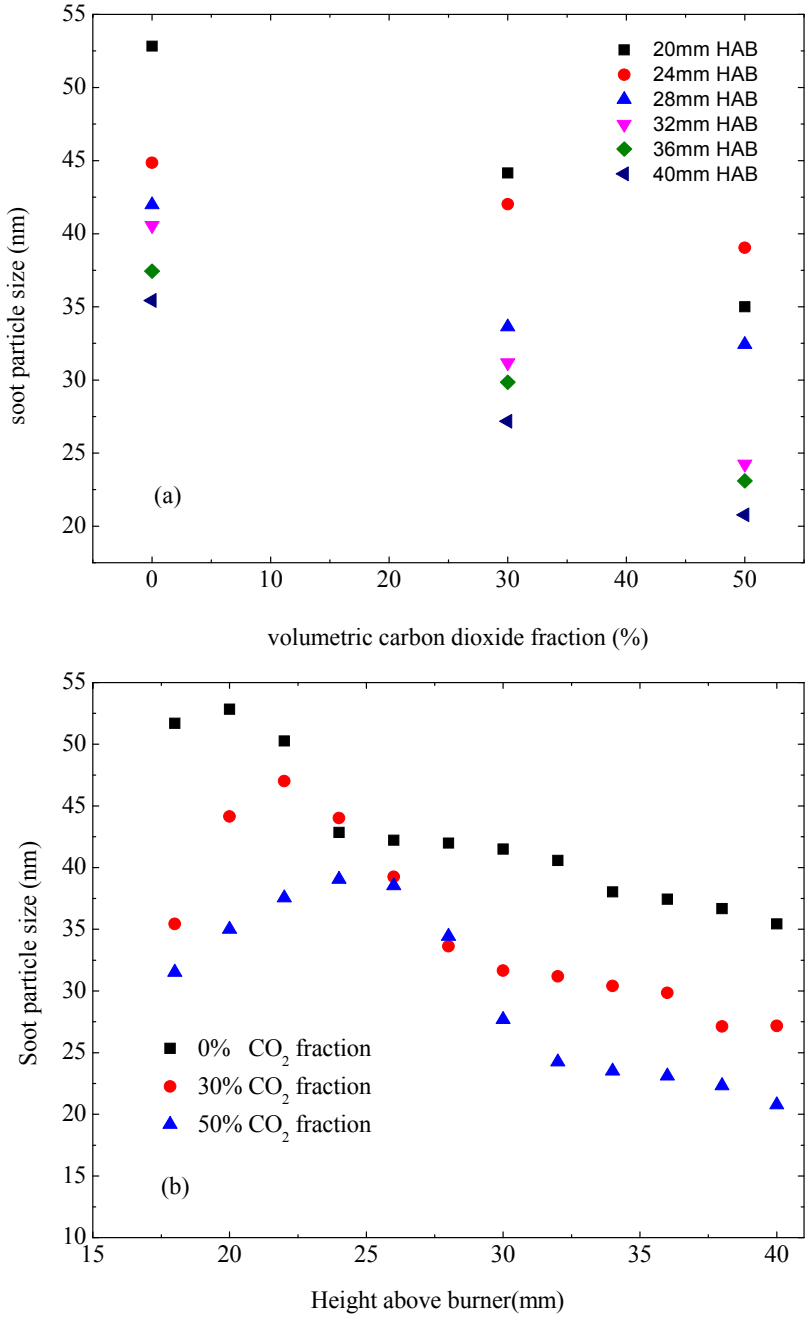

Fig. 9. Calculated particle sizes in different flames. (a) The relation between particle sizes and volumetric CO_2 fraction of CO_2. (b) The relation between particle sizes and the height above the burner.

absorption function was acquired through the plotting of fluence curves, and soot particle sizes were measured by temporal LII signals.

The luminous flame height decreased with the CO_2 addition, while the height of the dark region increased. It is thus concluded that CO_2 addition to the fuel side slowed down the nucleation rate and thus compressed the formation of nascent soot

A slight decrease in the absorbency of soot particles was observed. This indicates that CO_2 dilution made soot particles less mature. From the results of the particle size measurement, it was concluded that adding CO_2 to the fuel side reduced the particle sizes and changed the boundary between the surface growth region and the oxidation region of flames.

ACKNOWLEDGMENTS

This work was supported by the Natural Science Foundation of China (No. 51206144), a public project of the Ministry of Environmental Protection (201409008-4), the National Basic Research Program of China (2015CB251501), and the Program of Introducing Talents of Discipline to University (B08026).

REFERENCES

Angrill, O., Geitlinger, H., Streibel, T., Suntz, R. and Bockhorn, H. (2000). Influence of exhaust gas recirculation on soot formation in diffusion flames. *Proc. Combust. Inst.* 28: 2643–2649.

Barone, A.C., D'Alessio, A. and D'Anna, A. (2003). Morphological characterization of the early process of soot formation by atomic force microscopy. *Combust. Flame* 132: 181–187.

Bladh, H., Johnsson, J., Olofsson, N.E., Bohlin, A. and Bengtsson, P.E. (2011). Optical soot characterization using two-color laser-induced incandescence (2C-LII) in the soot growth region of a premixed flat flame. *Proc. Combust. Inst.* 33: 641–648.

Chen, L., Wu, J., Yan, M., Wu, X., Gréhan, G. and Cen, K. (2017). Determination of soot particle size using time-gated laser-induced incandescence images. *Appl. Phys. B* 123: 96.

D'Anna, A., D'Alessio, A. and Kent, J. (2002). Reaction path analysis of the formation of aromatics and soot in a coflowing laminar diffusion flame of ethylene. *Combust. Sci. Technol.* 174: 279–294.

Das, S.K. (2015). Fog-induced changes in optical and physical properties of transported aerosols over Sundarban, India. *Aerosol Air Qual. Res.* 15: 1201–1212.

Fan, M., Chen, L., Li, S., Zou, M., Su, L. and Tao, J. (2016). The effects of morphology and water coating on the optical properties of soot aggregates. *Aerosol Air Qual. Res.* 16: 1315–1326.

Gu, M., Chu, H. and Liu, F. (2016). Effects of simultaneous hydrogen enrichment and CO_2 dilution of fuel on soot formation in an axisymmetric coflow laminar ethylene/air diffusion flame. *Combust. Flame* 166: 216–228.

Jose, S. (2016). Characterisation of absorbing aerosols using ground and satellite data at an urban location, Hyderabad. *Aerosol Air Qual. Res.* 16: 1427–1440.

Lehre, T., Jungfleisch, B., Suntz, R. and Bockhorn, H. (2003). Size distributions of nanoscaled particles and gas temperatures from time-resolved laser-induced-incandescence measurements. *Appl. Opt.* 42: 2021–2030.

Lin, C.C., Yang, L.S. and Cheng, Y.H. (2016). Ambient $PM_{2.5}$, black carbon, and particle size-resolved number concentrations and the Ångström exponent value of aerosols during the firework display at the Lantern Festival in southern Taiwan. *Aerosol Air Qual. Res.* 16: 373–387.

Liu, F.S., Guo, H.S., Smallwood, G.J. and Gulder, O.L. (2001). The chemical effects of CO_2 as an additive in an ethylene diffusion flame: Implications for soot and NO_x formation. *Combust. Flame.* 125: 778–787.

Liu, F., Daun, K.J., Snelling, D.R. and Smallwood, G.J. (2006). Heat conduction from a spherical nano-particle: Status of modeling heat conduction in laser-induced incandescence. *Appl. Phys. B* 83: 355–382.

Mclintock, I.S. (1968). Effect of various diluents on soot production in laminar ethylene diffusion flames. *Combust. Flame.* 12: 217–225.

Michelsen, H.A., Liu, F., Kock, B.F., Bladh, H., Boiarciuc, A., Charwath, M., Dreier, T., Hadef, R., Hofmann, M., Reimann, J., Will, S., Bengtsson, P.E., Bockhorn, H., Foucher, F., Geigle, K.P., Mounaim-Rousselle, C., Schulz, C., Stirn, R., Tribalet, B. and Suntz, R. (2007). Modeling laser-induced incandescence of soot: A summary and comparison of LII models. *Appl. Phys. B* 87: 503–521.

Michelsen, H.A. (2017). Probing soot formation, chemical and physical evolution, and oxidation: A review of in situ diagnostic techniques and needs. *Proc. Combust. Inst.* 36: 717–735.

Migliorini, F., De Iuliis, S., Maffi, S. and Zizak, G. (2015). Saturation curves of two-color laser-induced incandescence measurements for the investigation of soot optical properties. *Appl. Phys. B* 120: 417–427.

Nagy, A., Czitrovszky, A., Kerekes, A., Veres, M. and Szymanski, W. W. (2016). Real-time determination of absorptivity of ambient particles in urban aerosol in Budapest, Hungary. *Aerosol Air Qual. Res*. 16: 1–10.

Oh, K.C., Do Lee, U., Shin, H.D. and Lee, E.J. (2005). The evolution of incipient soot particles in an inverse diffusion flame of ethene. *Combust. Flame* 140: 249–254.

Oh, K.C. and Shin, H.D. (2006). The effect of oxygen and CO_2 concentration on soot formation in non-premixed flames. *Fuel* 85: 615–624.

Olofsson, N., Johnsson, J., Bladh, H. and Bengtsson, P. (2013). Soot sublimation studies in a premixed flat flame using laser-induced incandescence (LII) and elastic light scattering (ELS). *Appl. Phys. B* 112: 333–342.

Pu, W. (2015). Size distribution and optical properties of particulate matter (PM_{10}) and black carbon (BC) during dust storms and local air pollution events across a loess plateau site. *Aerosol Air Qual. Res.* 15: 2212–2224.

Roper, F.G. (1977). Prediction of laminar jet diffusion flame sizes. 1. theoretical-model. *Combust. Flame* 29: 219–226.

Roper, F.G., Smith, C. and Cunningham, A.C. (1977). Prediction of laminar jet diffusion flame sizes. 2. experimental-verification. *Combust. Flame* 29: 227–234.

Schug, K.P., Manheimertimnat, Y., Yaccarino, P. and Glassman, I. (1980). Sooting behavior of gaseous hydrocarbon diffusion flames and the influence of additives. *Combust. Sci. Technol.* 22: 235–250.

Schulz, C., Kock, B. F., Hofmann, M., Michelsen, H., Will, S., Bougie, B., Suntz, R. and Smallwood, G. (2006). Laser-induced incandescence: Recent trends and current questions. *Appl. Phys. B* 83: 333–354.

Smooke, M.D., Mcenally, C.S., Pfefferle, L.D., Hall, R.J. and Colket, M.B. (1999). Computational and experimental study of soot formation in a coflow, laminar diffusion flame. *Combust. Flame* 117: 117–139.

Smooke, M.D., Long, M.B., Connelly, B.C., Colket, M.B. and Hall, R.J. (2005). Soot formation in laminar diffusion flames. *Combust. Flame.* 143: 613–628.

Sun, Z.W., Gu, D.H., Nathan, G.J., Alwahabi, Z.T. and Dally, B.B. (2015). Single-shot, Time-Resolved planar laser-induced incandescence (TiRe-LII) for soot primary particle sizing in flames. *Proc. Combust. Inst.* 35: 3673–3680.

Sunderland, P.B., Krishnan, S.S. and Gore, J.R. (2004). Effects of oxygen enhancement and gravity on normal

and inverse laminar jet diffusion flames. *Combust. Flame* 136: 254–256.

Vander Wal, R.L., Ticich, T.M. and Stephens, A.B. (1998). Optical and microscopy investigations of soot structure alterations by laser-induced incandescence. *Appl. Phys. B* 67: 115–123.

Wang, H. (2011). Formation of nascent soot and other condensed-phase materials in flames. *Proc. Combust. Inst.* 33: 41–67.

Will, S., Schraml, S., Bader, K. and Leipertz, A. (1998). Performance characteristics of soot primary particle size measurements by time-resolved laser-induced incandescence. *Appl. Opt.* 37: 5647–5658.

Wu, J., Chen, L., Zhou, J., Wu, X., Gao, X., Grehan, G. and Cen, K. (2017). Particle size distribution of soot from a laminar/diffusion flame. *Aerosol Air Qual. Res.* 17: 2095–2109.

Wu, L., Kobayashi, N., Li, Z. and Huang, H. (2016). Experimental study on the effects of hydrogen addition on the emission and heat transfer characteristics of laminar methane diffusion flames with oxygen-enriched air. *Int. J. Hydrogen Energy* 41: 2023–2036.

Wu, Y. (2015). Spectral light absorption of ambient aerosols in urban Beijing during summer: An intercomparison of measurements from a range of instruments. *Aerosol Air Qual. Res.* 15: 1178–1187.

Zhan, C., Zhang, J., Cao, J., Han, Y., Wang, P., Zheng, J., Yao, R., Liu, H., Li, H. and Xiao, W. (2016). Characteristics and sources of black carbon in atmospheric dustfall particles from Huangshi, China. *Aerosol Air Qual. Res.* 16: 2096–2106.

Zhao, H., Stone, R. and Williams, B. (2014). Investigation of the soot formation in ethylene laminar diffusion flames when diluted with helium or supplemented by hydrogen. *Energy Fuels* 28: 2144–2151.

Received for review, August 15, 2017
Revised, September 13, 2017
Accepted, September 13, 2017